International Journal of Radiation Oncology biology • physics

www.redjournal.org

Technological Advances

Proton Minibeam Radiation Therapy Reduces Side Effects in an In Vivo Mouse Ear Model

Stefanie Girst, MS,* Christoph Greubel, PhD,* Judith Reindl, MSc,* Christian Siebenwirth, MS,*,† Olga Zlobinskaya, PhD,† Dietrich W.M. Walsh, MSc,*,† Katarina Ilicic, MSc,† Michaela Aichler, PhD,‡ Axel Walch, PhD,‡ Jan J. Wilkens, PhD,† Gabriele Multhoff, PhD,† Günther Dollinger, PhD,* and Thomas E. Schmid, PhD†

**Institut für Angewandte Physik und Messtechnik (LRT2), Universität der Bundeswehr München, Neubiberg, Germany; †Department of Radiation Oncology, Klinikum rechts der Isar, Technische Universität München, Munich, Germany; and ‡Research Unit Analytical Pathology, Helmholtz Zentrum München, German Research Center for Environmental Health, Oberschleißheim, Germany*

Received May 20, 2015, and in revised form Sep 7, 2015. Accepted for publication Oct 8, 2015.

Summary

Proton minibeam radiation therapy is a novel implementation of spatial fractionation for normal tissue sparing that maintains tumor control by way of a homogeneous tumor dose using beam widening in tissue. The side effects of minibeam and homogeneous irradiation were compared in the ears of BALB/c mice at the same average dose of 60 Gy.

Purpose: Proton minibeam radiation therapy is a novel approach to minimize normal tissue damage in the entrance channel by spatial fractionation while keeping tumor control through a homogeneous tumor dose using beam widening with an increasing track length. In the present study, the dose distributions for homogeneous broad beam and minibeam irradiation sessions were simulated. Also, in an animal study, acute normal tissue side effects of proton minibeam irradiation were compared with homogeneous irradiation in a tumor-free mouse ear model to account for the complex effects on the immune system and vasculature in an in vivo normal tissue model.

Methods and Materials: At the ion microprobe SNAKE, 20-MeV protons were administered to the central part (7.2×7.2 mm^2) of the ear of BALB/c mice, using either a homogeneous field with a dose of 60 Gy or 16 minibeams with a nominal 6000 Gy (4×4 minibeams, size 0.18×0.18 mm^2, with a distance of 1.8 mm). The same average dose was used over the irradiated area.

Results: No ear swelling or other skin reactions were observed at any point after minibeam irradiation. In contrast, significant ear swelling (up to fourfold), erythema, and

Reprint requests to: Stefanie Girst, MS, Institut für Angewandte Physik und Messtechnik (LRT2), Universität der Bundeswehr München, Neubiberg 85579, Germany. Tel: (89) 6004-3506; E-mail: stefanie.girst@unibw.de

This work was supported by the Deutsche Forschungsgemeinschaft-Cluster of Excellence "Munich-Centre for Advanced Photonics," the Bundesministerium für Bildung und Forschung (grants 01GU0823, 02NUK038A, and 02NUK031B), the European Union FP7 DoReMi Network of Excellence, the Marie Curie Actions—Initial Training Networks as an Integrating Activity Supporting Postgraduate Research with Internships in Industry and Training Excellence (European Commission contract no. 317169), the Support of Public and Industrial Research using Ion beam Technology, and the Maier Leibnitz Laboratory Munich.

Conflict of interest: none.

Supplementary material for this article can be found at www.redjournal.org.

Acknowledgments—We thank Christine Bayer for her help during the irradiation sessions, Sabine Reinhardt for her support with the Gafchromic film dosimetry, and the staff of Maier-Leibnitz-Laboratorium for operating the tandem accelerator.

Int J Radiation Oncol Biol Phys, Vol. 95, No. 1, pp. 234–241, 2016

http://dx.doi.org/10.1016/j.ijrobp.2015.10.020

Although the homogeneously irradiated ears developed significant swelling, erythema, desquamation, and loss of sebaceous glands, no acute side effects occurred after minibeam irradiation.

desquamation developed in homogeneously irradiated ears 3 to 4 weeks after irradiation. Hair loss and the disappearance of sebaceous glands were only detected in the homogeneously irradiated fields.

Conclusions: These results show that proton minibeam radiation therapy results in reduced adverse effects compared with conventional homogeneous broad-beam irradiation and, therefore, might have the potential to decrease the incidence of side effects resulting from clinical proton and/or heavy ion therapy.

Introduction

Worldwide, approximately 50% of all patients with cancer undergo radiation therapy (1, 2). However, despite technical improvements, the success of radiation therapy is still hampered by the severe side effects that develop in normal tissue. Radiation therapy with protons or heavy ions offers an important advantage compared with photons with respect to the dose distribution in the depth of the tissue. This allows a sharp decrease in the dose directly behind the tumor (3). However, proton and heavy ion irradiation also causes normal tissue damage and can induce the development of secondary cancer, with detrimental effects on the patient's well-being after radiation therapy. New technologies such as microbeam radiation therapy (MRT), which was developed at Brookhaven National Laboratory (4) and the European Synchrotron Radiation Facility (5-8), and proton microchannel radiation therapy, developed at the ion microprobe SNAKE (Superconducting Nanoprobe for Applied nuclear [Kern] physics Experiments) in Munich (9), have provided implementations of spatial fractionation, with the aim of reducing normal tissue damage in the entrance channel. However, these 2 methods have shown differences in the irradiation of the tumor. X-ray MRT leads to an inhomogeneous dose distribution through the preserved microarray geometry. In contrast, proton microbeam or minibeam radiation therapy results in a homogeneous dose distribution in the tumor, similar to conventional broad beam irradiation (9, 10). The initially micrometer-size, or at least submillimeter, proton beams spread with increasing track length owing to interactions with the traversed tissue or their initial divergence, resulting in a homogeneous dose distribution within the tumor tissue when the minibeam distances have been adjusted accordingly (Fig. 1).

First experimental evidence with proton microbeams in an in vitro 3-dimensional human skin model demonstrated reduced negative irradiation effects of microchannel irradiation compared with a homogeneous broad beam irradiation (9). In that comparative in vitro study, greater cell viability and lower genetic damage was demonstrated using the MTT

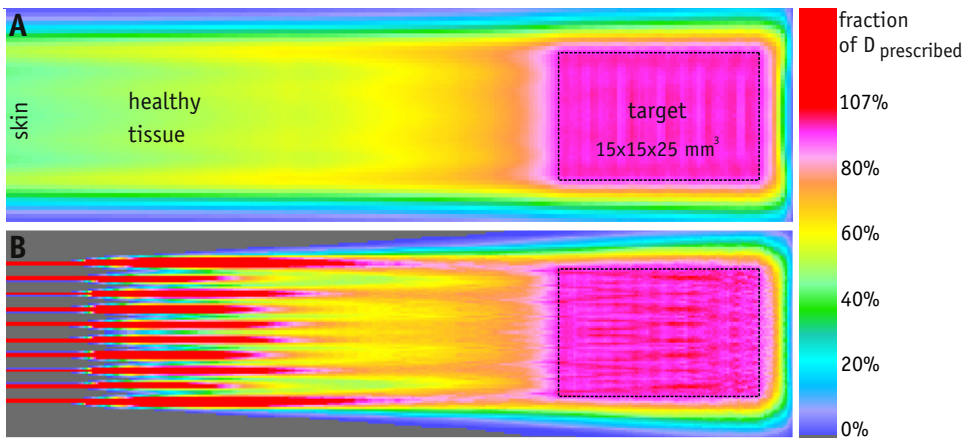

Fig. 1. Simulated dose distributions for homogeneous broad beam (A) and minibeam (B) irradiation of a model target volume, size 2.5 × 1.5 × 1.5 cm^3 at a depth of 7 to 9.5 cm underneath the surface from 1 direction (beams coming from the left). Homogeneous irradiation uses Gaussian pencil beams with a full width at half maximum size of ~4.2 mm, which already overlap in the skin. Minibeam irradiation uses Gaussian pencil beams of full width half maximum ~0.18 mm, which are arranged on the same square grid with an interbeam distance of 1.8 mm. The dose in the minibeams exceeded the tumor dose (prescribed dose [$D_{prescribed}$]; eg, with a factor of about 10-20 in the skin; doses ≥107% of the prescribed dose are red on the color bar), with nearly no dose in between. The dose distributions were calculated using an open-source planning system, CERR (11) and an additional proton dose algorithm (12) using Monte Carlo-generated pencil beams. Note minibeam shape was square instead of Gaussian in the experiment, leading to greater maximum doses in the skin than in the simulation.

(3-(4,5-dimethylthiazol-2-yl)-2,5-diphenyltetrazolium bromide) tissue viability and micronuclei assays, with a reduced and shorter inflammatory response, measured as the release of inflammatory cytokines in the culture medium of the skin (9).

For future therapeutic applications of this method, larger beam sizes and thus larger interbeam distances might be favored owing to the greater feasibility of creating "proton minibeams" with a full width at half maximum (FWHM) in the range of 0.1 to 1 mm rather than microbeams, for as long as a homogeneous irradiation of deep lying tumors is obtained from the laterally spreading proton beams. The proton beams spread laterally with increasing depth in tissue due to multiple coulomb scattering, leading to a homogeneous dose distribution in a deep lying tumor if the beam distances are chosen appropriately. Studies using larger beam sizes and interbeam distances have shown similar reduced side effects in an artificial in vivo model (13, 14). However, clinically relevant proof-of-concept results can only be obtained using proton minibeam irradiation in an animal model in which the complexity of irradiation effects, including the response of the vasculature and immune system, can be analyzed.

In the present experiments, the acute side effects of proton minibeam irradiation were compared with those of conventional homogeneous proton irradiation of normal tissue in a validated mouse model. In this mouse model, the effects of minibeam irradiation to mouse ears were compared with those of homogeneous irradiation. The irradiation geometry was determined in a simulation for a human patient, such that it would fit the irradiation of a target volume at a depth of 7 to 9.5 cm from 1 direction. However, owing to the limited beam energy and mouse thickness, tumor irradiation was not a part of the present study. Regardless, the tumor control should not change between the homogeneous and minibeam applications, because in both cases, the dose distributions and, thus, the treatment conditions would be the same for the minibeam and normal proton therapy (Fig. 1).

The mean proton dose of 60 Gy applied in a single fraction was chosen because of the results from a pilot x-ray irradiation experiment using varying homogeneous doses in mouse ears. That pilot experiment showed serious inflammatory reactions at the 60-Gy dose. It should be noted that the minibeam shape was square instead of Gaussian in the experiment, which led to slightly higher maximum doses (in the skin) than in the simulation. The outcomes of these proof-of-concept studies provide the first basis for a future application of this novel radiation therapeutic approach in humans.

Methods and Materials

Animal model and ethical approval

The 10- to 12-week-old female BALB/c mice (Charles River Laboratories, Sulzfeld, Germany) were kept in a temperature-regulated animal facility exposed to a 12-hour light/dark cycle, with ad libitum access to food and water. The District Government of Upper Bavaria approved all animal experiments, which were performed in accordance with the animal welfare and ethical guidelines of our institutions.

BALB/c mice were used for the irradiation experiments of the ears because of their lack of pigmentation, the presence of only a few thin hairs on the ears, the relatively large size of approximately 1 cm in diameter and thickness of approximately 250 μm. These factors ensured a precise dose application and allowed for the detection of 20-MeV protons (range in water ~4.6 mm) in transmission.

Simulations

The dose distributions for homogeneous broad beam (Fig. 1a) and minibeam (Fig. 1b) irradiation of a model target volume with a size of $2.5 \times 1.5 \times 1.5$ cm^3 in a depth of 7 to 9.5 cm underneath the surface of a patient from 1 direction were simulated. The dose distributions were calculated using an open-source planning system computational environment for radiotherapy research and an additional proton dose algorithm using Monte Carlo-generated pencil beams. Figure 1a shows a possible conventional treatment plan using Gaussian pencil beams with an FWHM of ~4.2 mm in a matrix and a distance of 1.8 mm, leading to a homogenous dose distribution in the target and the skin. For the minibeam irradiation (Fig. 1b), the pencil beam size was reduced to an FWHM of 0.18 mm, keeping the same matrix irradiation geometry. Tissue sparing was optimized using a maximized interbeam distance of proton minibeams under the constraint of obtaining a homogeneous dose distribution within the tumor (ie, within 95% to 107% of the prescribed dose; Fig. 1). The irradiation techniques used the same total number of protons, leading to the same average target dose but different dose distributions in the healthy tissue in front of the target.

Irradiation conditions for the proton study

The beam dimensions and distances chosen for the study of normal tissue reactions to proton therapy corresponded to those required to treat a tumor with a homogeneous dose distribution lying at a depth of 7 cm below the skin, as described in the previous section. To investigate the acute side effects of minibeam radiation therapy in healthy tissue, a small animal model was chosen, without a tumor. The right ears of BALB/c mice were irradiated using a matrix with an interbeam distance of 1.8 mm, a square size of 0.18×0.18 mm^2, and nominal dose of 6000 Gy (Fig. 2; beam preparation provided in Appendix E1; available online at www.redjournal.org). This resulted in a mean dose across the irradiated area of 60 Gy. For comparison, a homogeneous proton irradiation at the same mean skin dose of 60 Gy was used and included the same number of protons in an irradiation field of 7.2×7.2 mm^2 (collimated

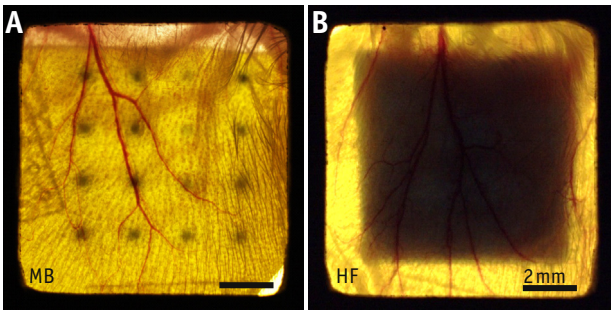

Fig. 2. Irradiation geometry of the mouse ear study. Photograph of Gafchromic film behind mouse ear immediately after irradiation with minibeams (MB) (0.18×0.18 mm^2) (A) and homogeneous field (HF) (B). Owing to the limited sensitivity range of the films, no absolute values of the irradiated high doses could be extracted from the images. Minibeam dimensions are enlarged due to beam widening in the ear.

beam, data provided in Appendix E1; available online at www.redjournal.org).

Thus, a matrix with the same interbeam distance of 1.8 mm was used in the animal experiment and our simulation (Fig. 1a). However, for ease of preparation, we used squares instead of Gaussian minibeams in the animal experiment. The mean skin dose of 60 Gy was determined in a pilot study with X rays to obtain strong reactions from the irradiation of the mouse ears in the homogenous cases (Appendix E1; available online at www.redjournal.org). The single fraction dose required to obtain similar normal tissue reactions would be lower in humans.

For a 90-day follow-up study, 12 BALB/c mice were irradiated with minibeams, 12 with a homogeneous field, and 10 with sham irradiation. The latter group served as the control group. Another 18 mice similarly underwent irradiation for histologic analysis at 15, 25, and 36 days after irradiation (3 mice per irradiation group [minibeam and homogeneous field] and measurement point).

Irradiation using 20-MeV protons was performed at the ion microprobe SNAKE, which has been adapted for biologic experiments using cells, tissues, and animals (15-17). A specially developed, temperature-controlled aluminum holder allowed for the irradiation of the central part of the right ear, with the rear of the ear facing the beam. With every proton traversing the ear (range ~4.6 mm much greater than ear thickness) and reaching a scintillator-photomultiplier detector positioned approximately 5 cm behind the ear, the dose could be calculated from the number of protons applied to a specific area on the skin and the linear energy transfer value (2.66 keV/μm at the ear). However, because of the required high particle count rates in the MHz range (to ensure irradiation times of <30 minutes and anesthesia time of <45 minutes), the dead time of the detector and the detection electronics (~15%-35%, depending on irradiation mode) had to be corrected using dosimetry with radiochromic films.

Irradiation was performed with the mice under general anesthesia, which was induced by intraperitoneal injection of medetomidine (0.5 mg/kg), midazolam (0.5 mg/kg), and fentanyl (0.05 mg/kg). The antagonist atipamezole (2.5 mg/kg), flumazenil (0.5 mg/kg), and naloxone (1.2 mg/kg) was administered subcutaneously that maximum 45 min after induction, the antagonist was administered.

Ear thickness measurements

During a 90-day follow-up period, the thickness of the treated right ear and the untreated left ear was measured regularly in triplicate using a specially adapted electronic external measuring gauge (C1X079; Kröplin GmbH, Schlüchtern, Germany), with measuring contacts 6 mm in diameter.

Skin reaction scoring

Acute skin reactions resulting after irradiation were monitored with regard to erythema, desquamation, changes in ear morphology, and hair loss. Hair loss was surveyed as an additional skin reaction in the mouse model. However, it was not added to the skin score of the inflammatory response. Therefore, this score only consisted of the 2 parts, erythema (score A) and desquamation (score B), which were simply summed to give a total skin score (Table 1, modified from [18]).

Histologic findings

The mice were euthanized at 15, 25, 36, and 90 days after irradiation, and the ears were dissected, fixed in formalin, and embedded in paraffin. Tissue sections were cut (3-μm thickness) and stained with hematoxylin and eosin for microscopic examination.

Results

Dose distributions for proton minibeams and homogeneous field irradiation

The homogeneous and minibeam irradiation modes are shown in Figure 2, using radiochromic film mounted

Table 1 Skin reaction scoring

Skin score	Description
Score A (erythema)	
0	No erythema
0.5	Mild erythema
1.5	Definite erythema
3	Severe erythema
Score B (desquamation)	
0	No
1	Dry desquamation
2	Crust
3	Moist desquamation

Data modified from Law et al (18).

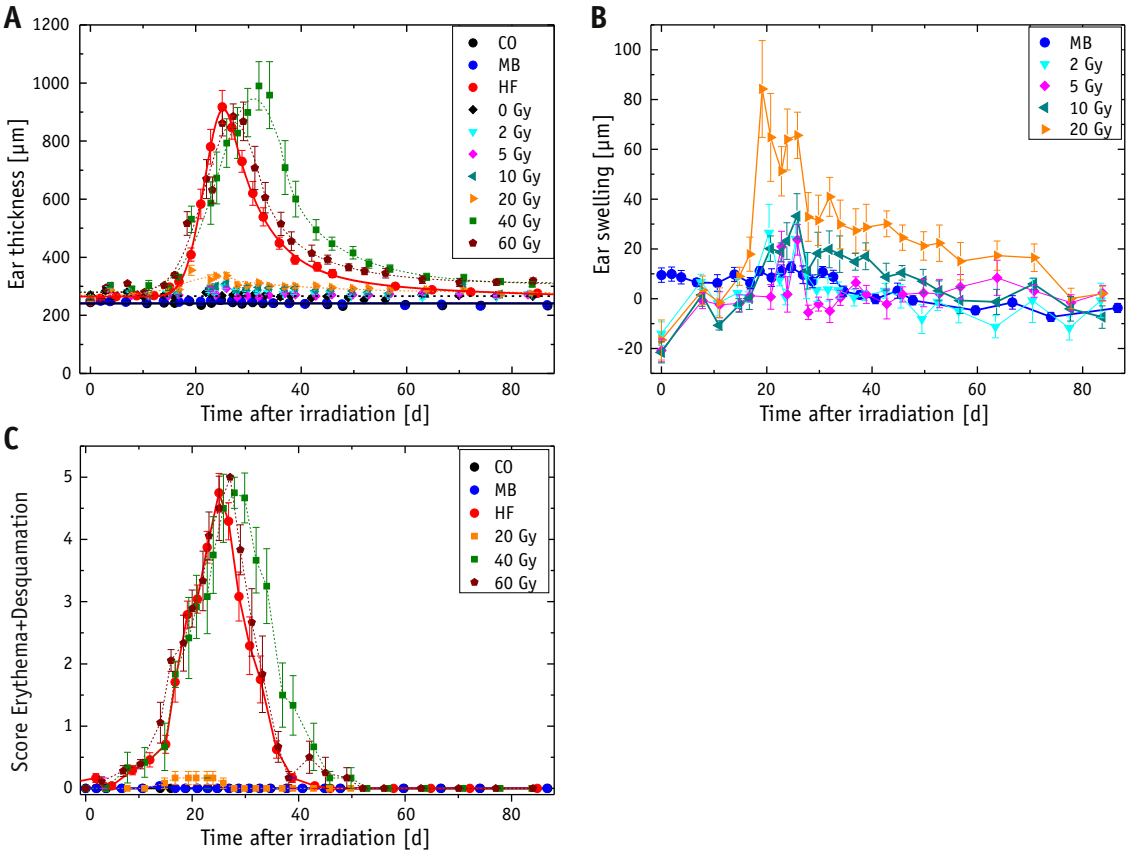

Fig. 3. Ear thickness (A), swelling (B), and skin reactions (C) after proton irradiation with minibeams (MB) and homogeneous field (HF) compared with x-ray irradiation. Ear swelling was determined as the difference in ear thickness between the irradiated (right) and unirradiated (left) ears and was only displayed for comparison of minibeam irradiation with low x-ray doses. The skin score is the sum of the erythema and desquamation score (Table 1). *Abbreviation:* CO = control group.

behind the mouse ear during irradiation (no absolute doses are identifiable owing to the saturation effects). Quantitative characterization of the irradiation fields in the 2 modes was also done with radiochromic films (Gafchromic EBT3 [19]) mounted at the mouse ear position (without the mouse ear). The number of applied protons had to be downscaled to fit the sensitivity range of the film. The mean doses of the 2 irradiation modes were in good agreement with the prescribed dose of 60 Gy: mean 59 ± 5 Gy for the minibeam irradiation mode and 58 ± 6 Gy for the homogeneous mode. The dose uncertainty mainly resulted from the radiochromic film dosimetry to correct for the detector dead times at the required high count rates and the uncertainty of the field sizes.

Ear swelling

The ears irradiated with minibeams showed no increase in ear thickness at any time after irradiation within the measurement accuracy of about 10% to 15% (Fig. 3a; Fig. E3; available online at www.redjournal.org). In contrast, homogeneous irradiation led to significant ear swelling of ≤4 times the initial thickness (ie, >1 mm). The maximum of the average thickness was reached approximately 4 weeks (days 25-26) after irradiation; however, the individual curves differed in shape and peak among the 12 homogeneously irradiated mice. A comparison with the x-ray curves showed a very similar response for the ears irradiated homogeneously with 60 Gy with respect to the maximal thickness and time required for development. To determine the x-ray dose yielding an equivalent response to that of the minibeams, the ear swelling (ie, the difference between the right [irradiated] and left [unirradiated] ear; mean thickness of all measurements [left ear]) was determined to account for the different initial ear thicknesses between the proton and x-ray groups (Fig. 3b). Ear swelling after homogeneous x-ray irradiation with 10 Gy ($P<.01$) and 20 Gy ($P<.001$) was significantly greater than that of the minibeam irradiated mice from days 20 to 74 after irradiation. Irradiation with 2- and 5-Gy X rays did not produce significant swelling relative to the sham-irradiated controls or relative to the minibeam irradiation group ($P>.5$). In summary, these data indicate that minibeam irradiation with a mean dose of 60 Gy induces less ear swelling than homogeneous x-ray irradiation at 10 Gy (Table 2).

Table 2 Summary of results for all endpoints

Endpoint	Homogeneous field	Minibeams	Minibeam equivalent x-ray dose (Gy)
Ear swelling	Up to fourfold	No	<10
Erythema	Severe	No	<20
Desquamation	Crust and moistness	No	<40
Changes in ear morphology	Waviness, bending, stiffness	No	<40
Hair loss	In irradiation field	No	<40
Histologic findings	Loss of sebaceous glands, inflammation, fibrosis, enlargement of epidermis	No changes visible	NA

Abbreviation: NA = not applicable.

Ear skin reactions

Erythema, desquamation, and other skin reactions such as hair loss were monitored at the same regular intervals as the monitoring of the ear thickness. Because the temporal development was very similar for erythema and desquamation, both scores (Table 1) were summed to obtain a single score for the acute inflammatory response after irradiation (Fig. 3c). For the homogeneously irradiated ears, mild skin reddening occurred first around day 9 after irradiation, and dry desquamation began about 17 days after radiation therapy. The maximum skin score, in the presence of definite to severe erythema, crust formation, and even partial moist desquamation, was reached more or less simultaneously with the date of maximum ear swelling, about 25 days after irradiation. These symptoms returned to normal levels from about day 46 onward. A comparison with the x-ray data displayed very similar behavior for ears irradiated homogeneously with 60-Gy protons and X rays. Furthermore, changes in the ear morphology, such as waviness, bending, and stiffness, were detected in several of the homogeneously irradiated ears. A loss of hair in the irradiated field first became visible at the decline of desquamation about 4 to 5 weeks after irradiation.

However, no visible skin reaction or hair loss was detected at any measurement point after proton minibeam irradiation, identifiable by the constant skin score of 0 in Figure 3c. This corresponded to the response of the ears irradiated with x-ray doses of $\leq$10 Gy, and 20 Gy resulted in a measurable increase in the skin score (mainly mild erythema).

Histologic findings

Representative examples of the histologic sections of the mouse ears are shown in Figure 4. No noticeable changes were found in any skin samples of the minibeam-irradiated mouse ears at all analyzed measurement points. Because it is almost impossible to ensure a cut directly through 1 of the minibeams, it could not be excluded that changes had occurred directly in the irradiated spots. However, most of the skin area after microbeam irradiation was unchanged. The histologic findings of samples taken 15 days to 3 months after homogenous irradiation differed significantly from their corresponding controls. From day 15 onward, the sebaceous glands were missing in the irradiated field but not in the surrounding skin and did not recover until day 90. At the time of the highest skin score around day 25, significant swelling of the epidermis was found in both skin layers, accompanied by inflammation and fibrosis. The decrease in the measured ear thickness at day 36 correlated well with a decrease in the swelling of the epidermis and a decline in the fibrotic area, as displayed in the histologic sections. No change in the abundance and appearance of the hair follicles was detected in the homogeneously irradiated ears at any point; however, the hair growth was still impeded 4 to 5 weeks after irradiation until the end of the observation period.

Discussion

In radiation therapy, the occurrence of normal tissue injury often limits the radiation dose that can be maximally applied to the tumor. Despite advanced treatment techniques with highly conformal treatment planning, skin reactions still occur in the irradiated region (20). The acute radiation effects of the skin often start as modest erythema and continue, becoming dry or confluent moist desquamation and leading to discomfort and pain (20). Necrosis and edema usually occur within 2 weeks after irradiation and result from cell death of keratinocytes in the epidermis (21). Moist desquamation occurs when clonogenic cells in the basal layer are destroyed and thus cannot replace the damaged tissue. Consequently, the epidermis becomes damaged (22), and inflammation occurs throughout the complete treatment period, healing only weeks after the end of the radiation therapy regimen. Acute skin reactions, which cause itchiness and pain, can be severe and can thus become dose-limiting reactions (20).

The aim of the present study was to compare the side effects of a homogeneous irradiation technique and a minibeam proton irradiation technique in an in vivo animal model at clinically relevant beam dimensions and distances. The present study provides important information toward implementation of this novel concept into clinical radiation

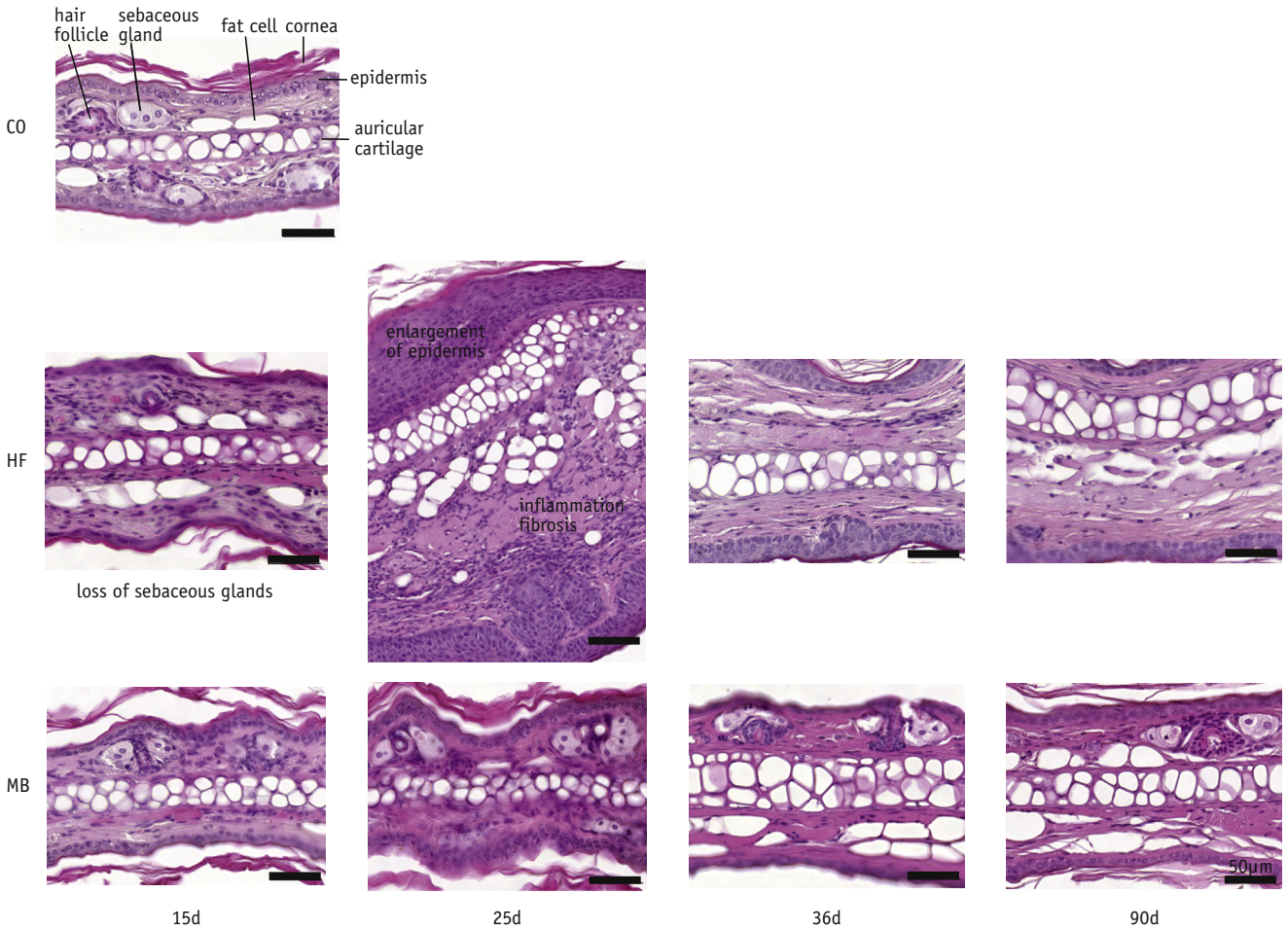

Fig. 4. Histologic findings of untreated (control group) ears and ears irradiated with homogeneous field (HF) and minibeams (MB) examined 15, 25, 36, and 90 days after irradiation (hematoxylin-eosin stain). No changes were found in the histologic features of the MB-irradiated ears. In contrast, HF irradiation led to a loss of sebaceous glands (from day 15), enlargement of the epidermis, inflammation, and fibrosis. The displayed sections of the MB-irradiated ears were not necessarily through the irradiated spots. Note, ears were necessarily from different mice.

therapy. An animal model was chosen to study the influence of this novel irradiation mode on the immune system, vasculature, and complete metabolism of a whole organism. The ear of adult BALB/c mice has a layer of skin tissue on each side of the cartilage (23), allowing examination of irradiation-induced reactions on both sides simultaneously.

Homogeneous irradiation with 60 Gy induced an up to fourfold increase in the ear thickness, and a high degree of edema in both skin layers was found on the histologic sections. However, no swelling could be detected at any point after minibeam irradiation at the same mean dose. Furthermore, no erythema, desquamation, or hair loss was visible in the mice irradiated with the proton minibeams. In contrast, those that received homogeneous proton irradiation developed all 3 side effects.

Histologic analysis also identified the loss of the sebaceous glands, inflammation, and fibrosis and significant enlargement of the epidermis only in the homogeneously irradiated tissue. In contrast, minibeam irradiation did not induce any significant changes in the morphology compared with the corresponding control group. A loss of sebaceous glands translates into loss of sebaceous secretion and a decrease in surface lipid levels and leads to a deterioration of the skin milieu. This can manifest itself in the form of dry and sensitive skin in the irradiated area (24).

An analysis of all endpoints showed that the acute side effects of proton minibeam radiation therapy at an average 60-Gy dose in BALB/c mouse ears only occurred with homogeneous x-ray doses of <10 Gy. These findings indicate a dose reduction factor >6. This result can either be directly translated into a reduction of side effects compared with broad beam irradiation at the same dose (required to control the tumor) or be used to enhance the dose within the tumor for radioresistant cancer types, maintaining the incidence and severity of normal tissue damage at a tolerable level. Furthermore, proton minibeam irradiation would allow for hypofractionation during radiation therapy, because normal tissue damage would not be the main limitation. However, in all cases, tumor control must be ensured

by a homogeneous dose distribution in the target volume using appropriate minibeam dimensions and distances. The maximum possible beam-to-beam distance depends on the tumor depth, with deeper lying tumors allowing for larger interbeam distances. All minibeams must widen sufficiently when approaching the tumor to form a homogeneous dose distribution in the target volume. Thus, protons reaching the distal edge of the target volume must have already spread sufficiently at the proximal edge to ensure a homogeneous dose distribution throughout the whole target volume. Similar approaches using minibeams for heavy ion therapy might also be beneficial; however, the distance, and thus the size, of the minibeams would have to be reduced compared with those of protons, owing to the smaller lateral spread of heavier ions. However, the technical realization of submillimeter ion beams remains to be elucidated.

Conclusions

The results from our animal study have clearly demonstrated that proton minibeam irradiation reduces the incidence of acute side effects compared with conventional broad beam irradiation in a mouse ear model and could therefore become an option in clinical proton therapy in the future.

References

1. Bernier J, Hall EJ, Giaccia A. Radiation oncology: A century of achievements. *Nat Rev Cancer* 2004;4:737-747.
2. Delaney G, Jacob S, Featherstone C, et al. The role of radiotherapy in cancer treatment: Estimating optimal utilization from a review of evidence-based clinical guidelines. *Cancer* 2005;104:1129-1137.
3. Paganetti H, Niemierko A, Ancukiewicz M, et al. Relative biological effectiveness (RBE) values for proton beam therapy. *Int J Radiat Oncol Biol Phys* 2002;53:407-421.
4. Slatkin DN, Spanne P, Dilmanian FA, et al. Subacute neuropathological effects of microplanar beams of x-rays from a synchrotron wiggler. *Proc Natl Acad Sci U S A* 1995;92:8783-8787.
5. Laissue JA, Blattmann H, Wagner HP, et al. Prospects for microbeam radiation therapy of brain tumours in children to reduce neurological sequelae. *Dev Med Child Neurol* 2007;49:577-581.
6. Serduc R, Christen T, Laissue J, et al. Brain tumor vessel response to synchrotron microbeam radiation therapy: A short-term in vivo study. *Phys Med Biol* 2008;53:3609-3622.
7. Brauer-Krisch E, Bravin A, Lerch M, et al. MOSFET dosimetry for microbeam radiation therapy at the European Synchrotron Radiation Facility. *Med Phys* 2003;30:583-589.
8. Brauer-Krisch E, Requardt H, Regnard P, et al. New irradiation geometry for microbeam radiation therapy. *Phys Med Biol* 2005;50:3103-3111.
9. Zlobinskaya O, Girst S, Greubel C, et al. Reduced side effects by proton microchannel radiotherapy: Study in a human skin model. *Radiat Environ Biophys* 2013;52:123-133.
10. Dilmanian FA, Eley JG, Krishnan S. Minibeam therapy with protons and light ions: Physical feasibility and potential to reduce radiation side effects and to facilitate hypofractionation. *Int J Radiat Oncol Biol Phys* 2015;92:469-474.
11. Deasy JO, Blanco AI, Clark VH. CERR: A computational environment for radiotherapy research. *Med Phys* 2003;30:979-985.
12. Schell S, Wilkens JJ. Advanced treatment planning methods for efficient radiation therapy with laser accelerated proton and ion beams. *Med Phys* 2010;37:5330-5340.
13. Girst S, Marx C, Bräuer-Krisch E, et al. Improved normal tissue protection by proton and x-ray microchannels compared to homogeneous field irradiation. *Phys Med* 2015;31:615-620.
14. Girst S, Greubel C, Reindl J, et al. The influence of the channel size on the reduction of side effects in microchannel proton therapy. *Radiat Environ Biophys* 2015;54:335-342.
15. Hauptner A, Dietzel S, Drexler GA, et al. Microirradiation of cells with energetic heavy ions. *Radiat Environ Biophys* 2004;42:237-245.
16. Greubel C, Hable V, Drexler GA, et al. Quantitative analysis of DNA damage response factors after sequential ion microirradiation. *Radiat Environ Biophys* 2008;47:415-422.
17. Greubel C, Assmann W, Burgdorf C, et al. Scanning irradiation device for mice in vivo with pulsed and continuous proton beams. *Radiat Environ Biophys* 2011;50:339-344.
18. Law MP, Ahier RG, Field SB. The response of mouse skin to combined hyperthermia and X-rays. *Int J Radiat Biol Relat Stud Phys Chem Med* 1977;32:153-163.
19. Reinhardt S, Hillbrand M, Wilkens JJ, et al. Comparison of Gafchromic EBT2 and EBT3 films for clinical photon and proton beams. *Med Phys* 2012;39:5257-5262.
20. Salvo N, Barnes E, van Draanen J, et al. Prophylaxis and management of acute radiation-induced skin reactions: A systematic review of the literature. *Curr Oncol* 2010;17:94-112.
21. Hopewell JW. The skin: Its structure and response to ionizing radiation. *Int J Radiat Biol* 1990;57:751-773.
22. Glean E, Edwards S, Faithfull S, et al. Intervention for acute radiotherapy induced skin reactions in cancer patients: The development of a clinical guideline recommended for use by the college of radiographers. *J Radiother Pract* 2000;2:75-84.
23. So P, Kim H, Kochevar I. Two-photon deep tissue ex vivo imaging of mouse dermal and subcutaneous structures. *Opt Express* 1998;3:339-350.
24. Grice EA, Segre JA. The skin microbiome. *Nat Rev Microbiol* 2011;9:244-253.